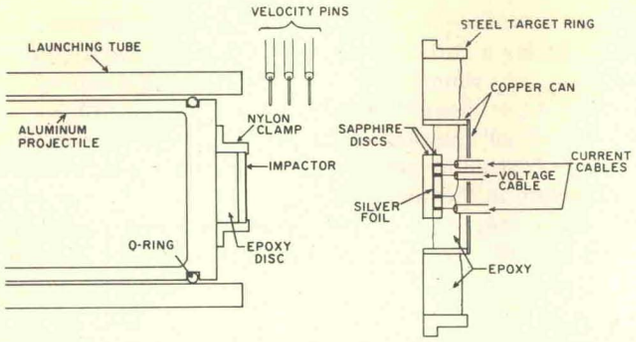

FIG. 2. Schematic diagram of impact configuration showing impactor and target assemblies.

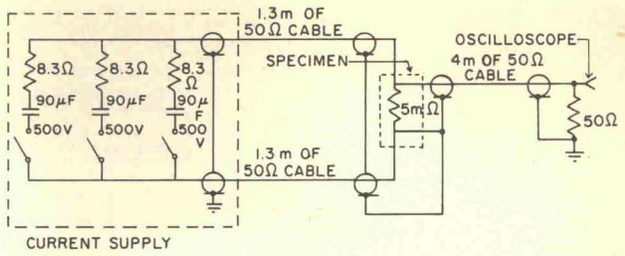

FIG. 3. Electronic measuring system.

tion would be anisotropic and mixed mode. But it has been determined experimentally that shock waves in sapphire propagate isotropically and in a pure longitudinal mode with an experimental uncertainty of $\pm 1\%$.[10] This is consistent with the experimental result that the elastic constants c_{11} and c_{33} happen to be of equal magnitude; its elastic response is symmetrical as a result.

The sapphire disk faces were parallel to within 2—10 μm. Faces were flat to within about 3 μm as observed with an optical flat and monochromatic light. As a check, the density of each sapphire disk was determined from weight measurements in air and water; the average value was 3.985 ± 0.005 g/cm^3.

Assembly involved wetting all pieces (sapphire and foil) with vacuum-outgassed epoxy (Shell Epon Resin 815). Foil leads were bent over the edges of a glass microscope slide and then pulled through the holes in the sapphire backing piece. The slide was then removed, and the front sapphire disk placed over the foil. This assembly was placed on a flat plate and screw pressure applied to a small Mylar-faced aluminum block placed on the sapphire backing piece. Lead holes were cleaned of epoxy using toothpicks soaked in acetone. After 2 h or more the holes were filled with dental amalgam which, compared to epoxy, provided a better shock-impedance match for silver and sapphire. The sandwich was visually inspected after curing to verify that the foil lay flat and to determine if there were air bubbles near the foil. The sandwich was then potted inside a copper ring which in turn had been potted into a target holding ring (Fig. 2). Next, a layer of aluminum was vacuum deposited on the target; this was done to provide a reflecting surface for optical alignment of the target on the end of the launching tube and to complete the electrical shielding with the copper ring and lid. Cables (RG-223/U) were attached and potted in place. Lengths of unshielded conductors from the plane of the foil to the coaxial cables were about 0.6 cm.

C. Impactors

Impactors for the first three shots were made of 6061-T6 aluminum. Extraneous signals were observed due to inductive coupling between sample and the metal projectile face. The remaining shots were done with a fused quartz or a sapphire impactor clamped to an aluminum projectile (Fig. 2). This eliminated inductive coupling. Impact misalignment was measured only in the first two shots. Tilt values recorded were 0.25 and 0.28 m. In the case of nonconducting impactors the projectile alignment was checked with an autocollimating telescope, the impactor face was perpendicular to the launching tube axis within 0.1—0.3 mrad. The sapphire target was also optically aligned to the tube axis. Actual tilt on impact was not recorded, since the small-diameter nonconducting impactors precluded such recording.

D. Recording system

The pulsed current source was a modified Pulsar model No. 301 power supply with three channels, each consisting essentially of a 90-μ capacitor, charged to 500 V, in series with 8.3 Ω (Fig. 3). The three channels were triggered simultaneously 15—30 μsec before impact.

Some recorded oscilloscope traces are shown in Fig. 4. One oscilloscope recorded the initial voltage step as well as voltage change across the foil upon shock compression. Two other oscilloscopes recorded only the voltage change due to shock compression. This was achieved by suppressing the initial voltage step using a differential comparator amplifier. The oscilloscopes used were 580 and 7000 series Tektronix, Inc. models; the system rise time was 4—5 nsec. Oscilloscope traces were recorded on Polaroid film. Horizontal and vertical calibrations on each shot were used to convert oscilloscope traces to voltage-time profiles

III. THEORY AND ANALYSIS

Flow of the analysis is shown in Fig. 5 and described below. From the experiment one obtains the impactor

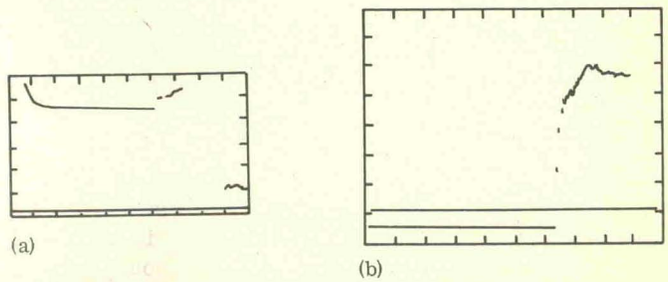

FIG. 4. Oscilloscope records. (a) Over-all record from shot 73-027 showing E_o and ΔE; 0.2 V/div, 3.5 μ sec/div. (b) Differential offset record from shot 73-050 showing ΔE vs time; 0.02 V/div, 0.2 μ sec/div.

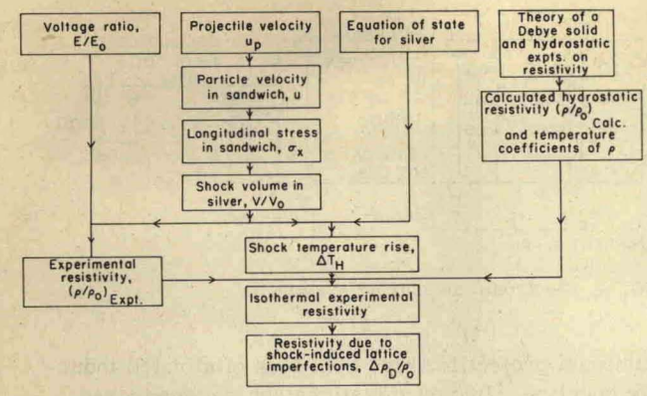

FIG. 5. Analysis flow chart.

velocity and a voltage-time profile of the shock response of the silver resistance. Known Hugoniot curves of silver and sapphire, and impactor velocity, are used to compute the pressure-volume state in silver.[11] (Computation is based on the Rankine-Hugoniot jump conditions for steady shocks.) Shock resistivity of silver is then computed. Using a P-V-T equation of state for silver fitted to experimental data, shock temperature is also calculated. Theory of a Debye solid is coupled with hydrostatic experiments on silver resistivity vs pressure to give an expression for the dependence of the temperature coefficient of resistivity on volume and to extrapolate the dependence of silver resistivity on hydrostatic pressure to 120 kbar. Then shock resistivity is corrected to isothermal conditions and compared to hydrostatic resistivity. Any deviation between shock and hydrostatic results is of interest.

A. Resistivity theory and analysis

In the Bloch-Gruneisen theory of electrical resistivity of metals[12]

$$\rho \propto T/\theta_R^2$$

for $T \gg \theta_R$ for the relation between resistivity ρ, absolute temperature T, and characteristic temperature θ_R. For an approximate treatment let us use

$$\rho = A(V)T/\theta^2(V) = \alpha(V)T, \tag{1}$$

where A is a catch-all parameter for the volume dependence of the electron band structure, Fermi geometry, Fermi energy, and details of the electron-phonon interaction, and α is the temperature coefficient of resistivity.

If we equate θ_R to θ_D, Debye temperature, then $d\ln\theta_D/d\ln V$ can be related to thermodynamic quantities, as was first noted by Gruneisen. The result is

$$\frac{d\ln\theta_D}{d\ln V} = \frac{V\alpha'}{C_V K_T} = \gamma(V), \tag{2}$$

where $\gamma(V)$ is the Gruneisen parameter, α' the volume coefficient of thermal expansion, K_T the isothermal compressibility, and C_V the constant volume specific heat.[13]

Let us consider the assumption $d\ln\theta_R/d\ln V = d\ln\theta_D/d\ln V$. Ziman[14] notes that Bloch resistivity theory is derived assuming scattering by longitudinal phonons only. So for a solid fitting the Bloch model we would expect $\theta_R = \theta_L$ which might be quite different from θ_D. Actually θ_R is close to θ_D for silver ($\theta_R = 219 \pm 20\,^\circ$K, $\theta_D = 228 \pm 3\,^\circ$K)[15] so that shear waves may participate in electron scattering processes to nearly the same extent that they do in thermal processes. Therefore, the assumption $d\ln\theta_R/d\ln V = d\ln\theta_D/d\ln V$ has some plausibility in the case of silver. Then the isothermal derivative of Eq. (1) becomes

$$\left(\frac{\partial\ln\rho}{\partial\ln V}\right)_T = 2\gamma(V) + \frac{d\ln A}{d\ln V}. \tag{3}$$

In this work we shall assume $d\ln A/d\ln V$ is constant over the range of compression studied

$$B \equiv \left.\frac{d\ln A}{d\ln V}\right|_{V=V_0} = \left(\frac{\partial\ln\rho}{\partial\ln V}\right)_{T,V=V_0} - 2\gamma(V_0).$$

Since the major dependence of ρ on volume for silver is contained in $\theta(V)$, this approximation should be adequate. Integration of Eq. (3) yields

$$\frac{\rho(V,T)}{\rho(V_0,T)} = \frac{\alpha(V)}{\alpha(V_0)} = \left(\frac{V}{V_0}\right)^B \exp\left(2\int_{V_0}^{V}\frac{\gamma(V')}{V'}dV'\right) = \left(\frac{V}{V_0}\right)^B\left(\frac{\theta}{\theta_0}\right)^{-2}. \tag{4}$$

Dugdale[16] used Bridgman's pressure derivatives for the resistance and found $B = -0.9$ for silver. Goree and Scott[17] also measured isothermal pressure derivatives of the resistivity of silver. They subtracted the pressure derivative of impurity resistivity to get the perfect lattice pressure derivative

$$\left(\frac{\partial\ln\rho_L}{\partial P}\right)_{T,P=1\text{atm}} = -4.2\times10^{-6}/\text{bar}.$$

Using Goree and Scott's derivative and $\gamma(V_0) = 2.43$, we found $B = -0.64$; this value of B was used for generating ρ on a hydrostat. [In finding $\gamma(V_0)$ ambient values of $K_T = 0.995\times10^{-6}$/bar, $\alpha' = 57.1\times10^{-6}/^\circ$K, and $C_V = 2.25$ bar cm^3/g were used.] Note that $(V/V_0)^B$, where $B<0$ tends to increase the resistivity on compression, while $(\theta/\theta_0)^{-2}$ decreases the resistivity on compression.

Experimentally metals do not exactly have resistivity proportional to absolute temperature; rather, the constant pressure resistivity is given by $\rho = \alpha T + \beta$ at high temperatures. So, to adjust theory to reality, assume $\rho = \alpha(V)T + \beta(V)$, where $\alpha(V) = A(V)/\theta^2(V)$ as before and $\beta(V)$ is an empirical parameter. From data of Kos[18] for silver $\alpha(V_0) = 0.005988$ $\mu\Omega$ cm/°K and $\beta(V_0) = -0.16$ $\mu\Omega$ cm for the range 150–300 °K.

For estimating the volume dependence of β, we use the Gruneisen-Borelius relation[19] for resistance R:

$$R_T/R_\theta = hT/\theta - (h-1), \quad h = 1.17.$$

This is an empirical relation for isotropic metals accurate in the range $0.2 < T/\theta < 1.2$. (For silver it is accurate at least to $T/\theta = 1.5$.) Ignoring thermal expansion we have $\rho_T/\rho_\theta = R_T/R_\theta$, and $\rho_T = h(T/\theta)\rho_\theta - (h-1)\rho_\theta$ in the form $\rho = \alpha T + \beta$. For silver $\rho_\theta = 1.18$